Electronic Supplementary Information (ESI)

MOF-74(Ni) Derived Partially Oxidized Ni@C Catalyst for SO_2 Electro-Oxidation Integrated with Solar Driven Hydrogen Evolution

Jin-Han Guo, [a] Xuming Wei [b] and Wei-Yin Sun* [a]

a Coordination Chemistry Institute, State Key Laboratory of Coordination Chemistry, School of Chemistry and Chemical Engineering, Nanjing National Laboratory of Microstructures, Collaborative Innovation Center of Advanced Microstructures, Nanjing University, Nanjing 210023, China. E-mail: sunwy@nju.edu.cn

b State Key Laboratory of Catalysis, Dalian Institute of Chemical Physics, Chinese Academy of Sciences, Dalian 116023, China

Characterization

Powder X-ray diffraction (PXRD) data were collected on a Bruker D8 Advance X-ray diffractometer with Cu Kα (λ = 1.5418 Å) radiation. The X-ray photoelectron spectroscopy (XPS) measurements were conducted using a Thermo Fisher Nexsa electron spectrometer using monochromated Al Kα radiation (*hv* = 1486.7 eV) as the excitation source. The XPS data were analyzed by the Avantage software package. Scanning electron microscope (SEM) observations were performed on a Hitachi S-4800 field emission scanning electron microscope at an accelerating voltage of 5 kV. The high-resolution transmission electron microscopy (HRTEM) images were acquired on JEOL JEM 2100F at 200kV accelerating voltage. The content of Ni was quantified by an Agilent 720ES ICP-OES.

Experimental Section

1) *Preparation of catalyst*

MOF-74(Ni) was synthesized according to the previous report.[1] 2,5-Dihydroxyterephthalic acid (H_4DOT, 0.9 g) and $Ni(NO_3)_2{\cdot}6H_2O$ (4.2 g) were sonicated and dissolved in 300 ml DMF,

18 ml EtOH, and 18 ml water. The mixture was transferred into 100 ml hydrothermal reactors and placed in an isothermal oven at 120 °C for 18 h. The resulting solid was washed with DMF twice and ethanol twice, then dried in the vacuum.

The MOF precursor was heated from room temperature to 900 °C at a heating rate of 5 °C min^{-1}, then pyrolyzed for 2 h in a N_2 atmosphere. Subsequently, the exposed nickel particles involved in the resultant product were removed by heating the samples in a 1 M HCl aqueous solution for 6 h at 70 °C. The black sample was collected by centrifugation, washed three times with distilled water, and dried in the vacuum to obtain the po-Ni@C catalyst.

2)*Preparation of catalytic inks*

The catalytic ink was prepared by mixing 5 mg of catalyst and 50 μl of 5% Nafion 117 (DuPont) into a water-isopropanol solution (1:1 vol) to a total volume of 1 ml. Then the mixture was sonicated for 1 h to form homogeneous inks. The catalytic cathode was prepared by drop-casting a certain amount of the catalyst ink onto a carbon fiber paper (TGP-H-060, Toray or W1S1009, CeTech) on a hot panel with a temperature of 150 °C, giving a catalyst loading of 0.5 mg cm^{-2}.

3) *Electrochemical tests*

Linear sweep voltammetry (LSV) and electrochemical active surface area (ECSA) measurements were performed in an H-cell. Carbon fiber paper (TGP-H-060, Toray) with electroactive area of 1 cm^2 coated with 0.5 mg cm^{-2} catalyst was used as the working electrode. A Nafion 117 membrane was used to separate the cell. A saturated calomel electrode was used as a reference, and a platinum plate was used as the counter electrode. An electrochemical workstation (CHI 730E) was employed. The Ohmic drops between the working and the

reference electrodes were measured by electrochemical impedance spectrum (EIS) at the open-circuit potential (OCP) and were 95% compensated by the electrochemical workstation. The electrode potentials were rescaled to RHE reference by $E_{RHE} = E_{SCE} + 0.0591\ V \times pH + 0.242\ V$. The anolyte was prepared by slowly adding 500 ml of 1 M Na_2SO_3 aqueous solution into 500 ml of 1 M H_2SO_4 aqueous solution with stirring. The formed aqueous solution of 0.5 M SO_2 (aq) with 0.5 M Na_2SO_4 support electrolyte has a pH of ~1.50 measured by a pH meter (PHS-25, Leici). A 0.5 M H_2SO_4 aqueous solution was utilized as the catholyte. The LSV curves were collected at a scan rate of 5 mV s^{-1}. The Tafel slope was calculated based on the Tafel equation [$\eta = b\log(j_{CO}/j_0)$] according to the LSV curve. The ECSA of po-Ni@C was determined by electrochemical double-layer capacity (EDLC) measurement in a 0.5 M H_2SO_4 aqueous solution, according to the reported EDLC value of graphene of ~21 mF cm^{-2}.[2] The thermal activation energy measurements were conducted under different temperatures controlled by a thermostatic bath.[3] The reaction orders were measured by LSV under a scan rate of 0.5 mV s^{-1} with different concentrations of SO_2 (aq). [4]

The stability test was performed in a custom-made flow-cell.[5, 6] The test was run under a constant current density of 20 mA cm^{-2} controlled by an electrochemical workstation (Im6ex, Zahner) for 24 h. A GDE with a 1 cm^{-2} active area (W1S1009) loaded with 0.5 mg cm^{-2} of the catalyst was utilized as the cathode. A proton exchange membrane (PEM, Nafion® 117) and a platinum plate counter electrode were sealed into the cell by the silica gel gaskets. The anode potential was measured at the end of each half-hour, and the Ohmic drops were manually compensated by measuring the resistance of the solution using the EIS function of the electrochemical workstation. The potentials were rescaled to RHE.

4) *Solar Driven HER with SO_2OR*

For the solar-driven hydrogen evolution measurements, a two-electrode setup was established in an H-cell and using a Pt mesh as HER electrode. The electrolytes are the same with LSV tests. A 300 W Xe arc lamp (Sirius-300P, Zolix Instruments) equipped with an AM 1.5G filter was utilized as the light source. A polysilicon solar cell (1 V, Zazr) was illuminated by the Xe lamp with an optical power density of 60 mW cm^{-2} to drive the electrolyzer. A series-connected electrochemical workstation (CHI730E) recorded the currents without applying any external bias.[7]

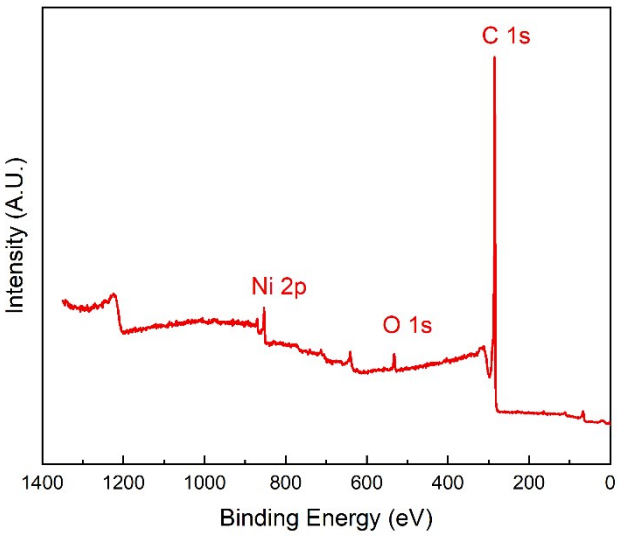

Fig. S1. XPS survey spectrum of po-Ni@C, the atomic contents of Ni, O, and C are 1.04 at%, 2.80 at%, and 96.14 at%, respectively.

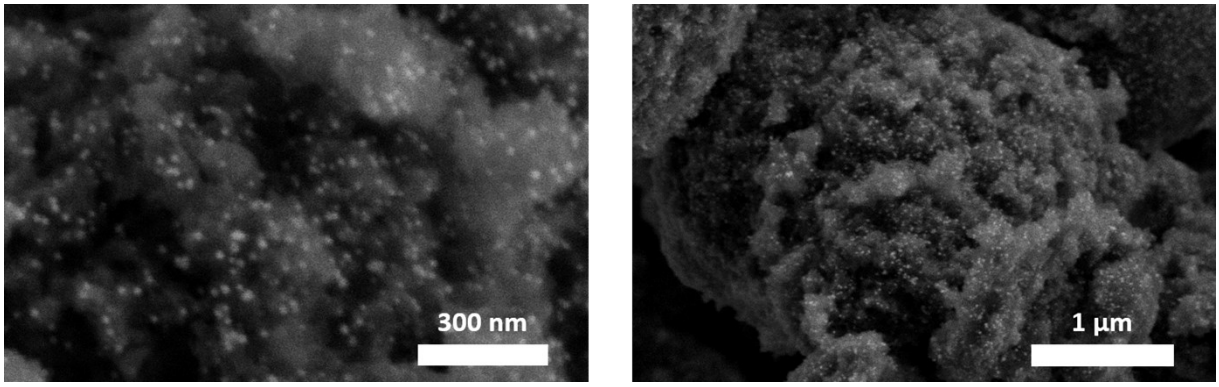

Fig. S2. SEM images of po-Ni@C.

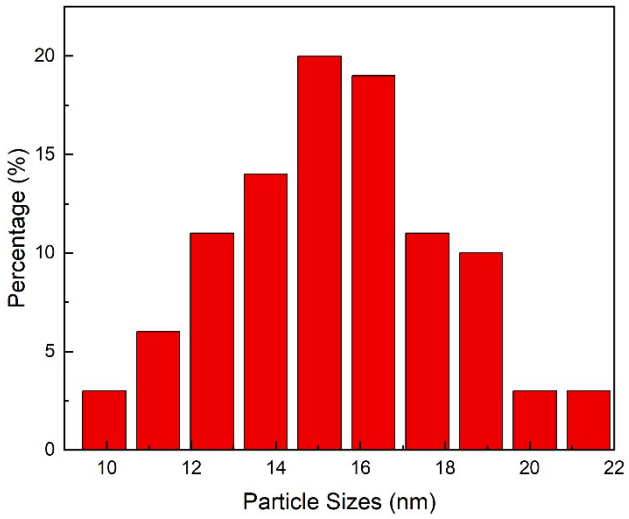

Fig. S3. Metallic particle size distribution in po-Ni@C.

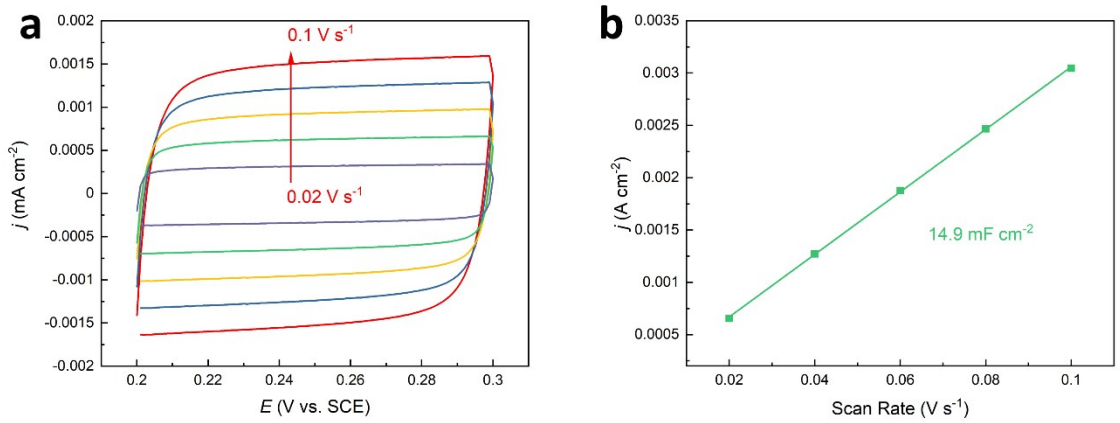

Fig. S4. ECSA measurements and double-layer capacitance of po-Ni@C.

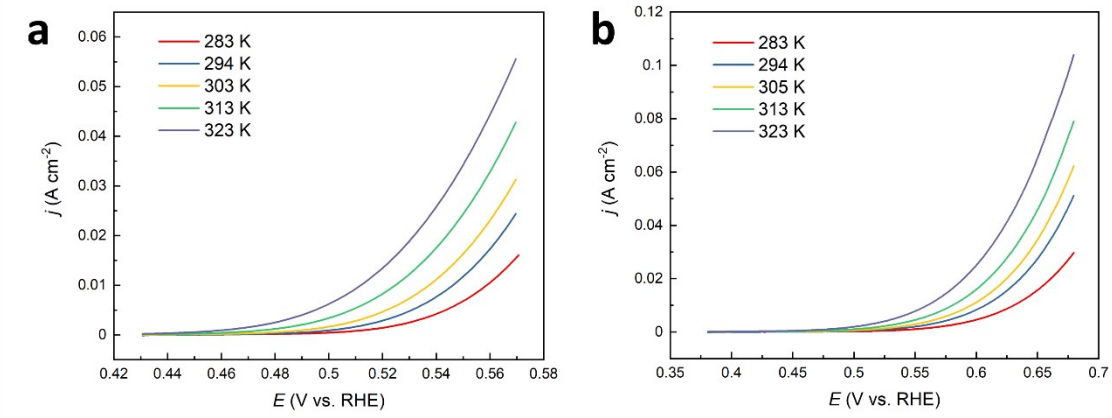

Fig. S5. LSV curves in the thermal activation energy measurements for po-Ni@C (a) and 20% Pt/C (b) catalysts.

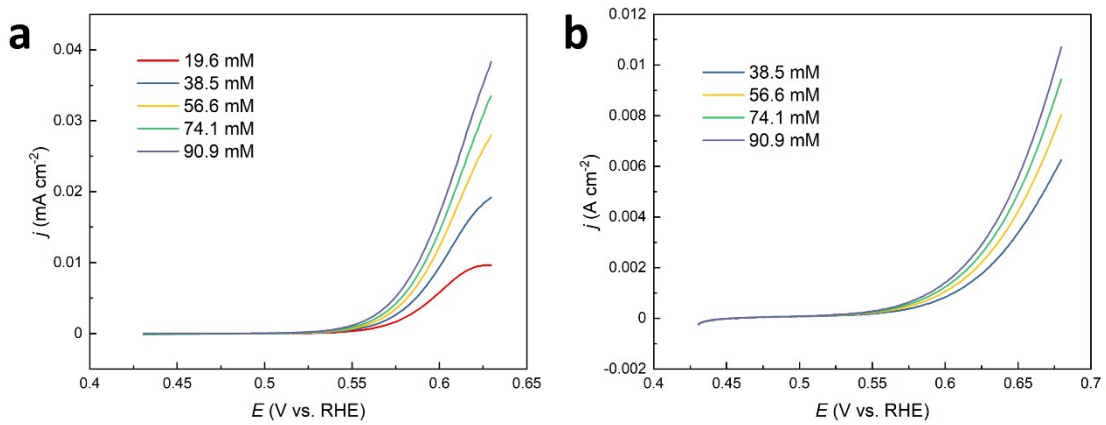

Fig. S6. LSV curves in the SO_2 reaction order measurements with different concentrations of SO_2 (aq) for po-Ni@C (a) and 20% Pt/C (b) catalysts.

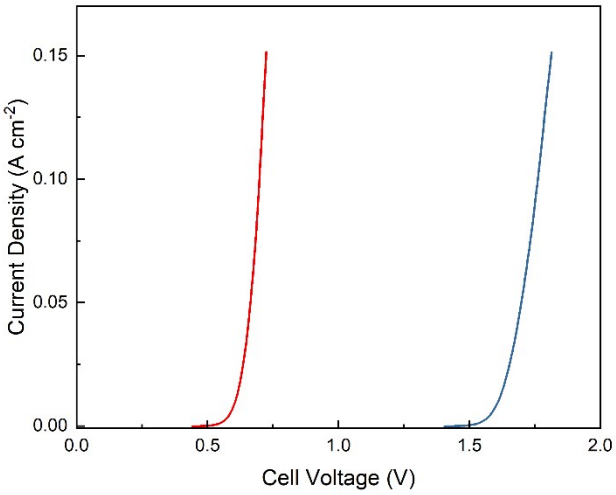

Fig. S7 The Ohmic drop corrected LSV curves of po-Ni@C catalyzed SO_2OR integrated H_2 production (red line) and Ti/IrO_2-Ta_2O_5 DSA mesh catalyzed whole water electrolysis (blue line).

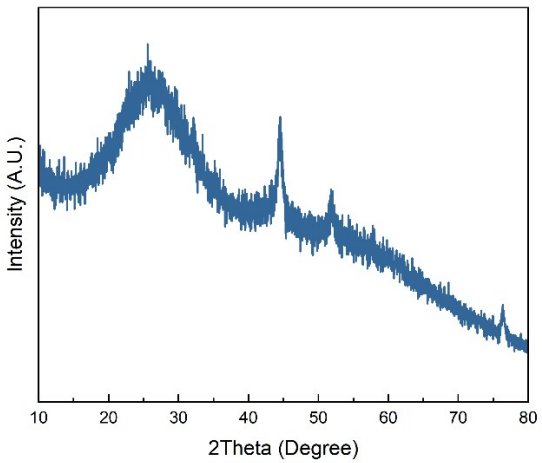

Fig. S8 PXRD pattern of po-Ni@C after catalysis.

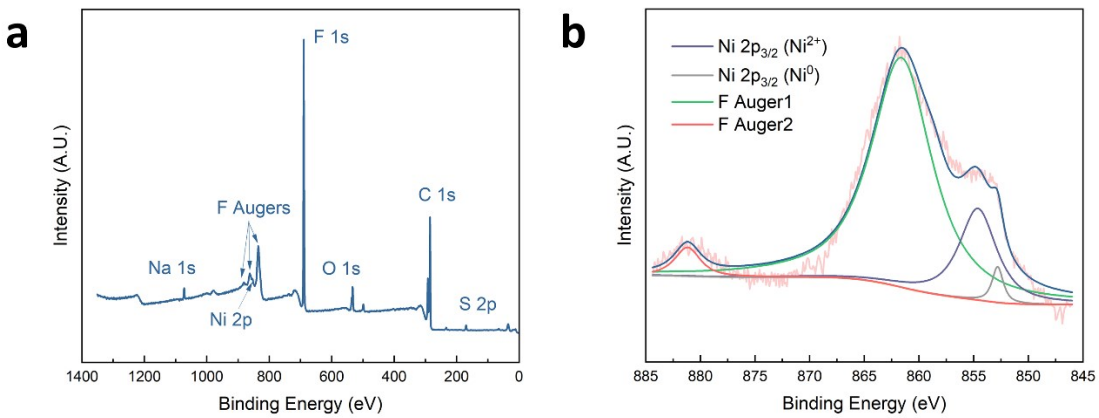

Fig. S9 (a) XPS survey spectrum of po-Ni@C after catalysis, the S 2p, F 1s, and Na 2s peaks are originated from the Nafion binder used in the electrode preparation. (b) Deconvoluted high-resolution XPS Ni 2p spectrum.

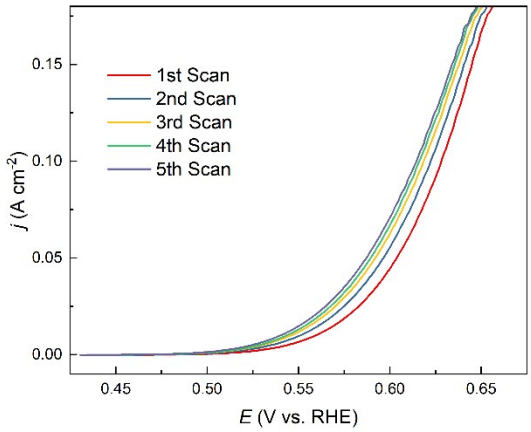

Fig. S10 The LSV curves during the activation process of the po-Ni@C catalyst.

Table S1 SO_2OR Efficiencies Comparison between po-Ni@C and other catalysts

Catalyst	*Onset Potential(V vs. RHE)*	*Tafel Slope(mV dec^{-1})*	*j_{max}(A cm^{-2})*	*Ref*
po-Ni@C	0.45	35	0.15	This Work
20% Pt/C	0.46	97	0.12	This Work
S/Poly-Pt	0.48	74	0.038	3
S/Poly-Au	0.50	~50	0.49	4
Doping (I)-Cu@N-C	0.52	~	0.001	8
Fe-N-Doped Carbon	0.50	~	0.001	9
Fe-N-C	0.50	~	0.001	10
Poly-Au	0.52	~	0.30	11
Poly-Pt	0.48	~	0.12	11

References:

1 L. J. Wang, H. Deng, H. Furukawa, F. Gandara, K. E. Cordova, D. Peri and O. M. Yaghi, *Inorg. Chem.*, 2014, **53**, 5881-5883.

2 T. Zheng, K. Jiang, N. Ta, Y. Hu, J. Zeng, J. Liu and H. Wang, *Joule*, 2019, **3**, 265-278.

3 J. A. O'Brien, J. T. Hinkley and S. W. Donne, *J. Electrochem. Soc.*, 2010, **157**, F111-F115.

4 J. A. O'Brien, J. T. Hinkley and S. W. Donne, *J. Electrochem. Soc.*, 2012, **159**, F585-F593.

5 J.-H. Guo and W.-Y. Sun, *Appl. Catal. B*, 2020, **275**, 119154.

6 J.-H. Guo, X.-Y. Zhang, X.-Y. Dao and W.-Y. Sun, *ACS Appl. Nano Mater.*, 2020, **3**, 2625-2635.

7 J. Gao, F. Sahli, C. Liu, D. Ren, X. Guo, J. Werner, Q. Jeangros, S. M. Zakeeruddin, C. Ballif, M. Grätzel and J. Luo, *Joule*, 2019, **3**, 2930-2941.

8 Q. Zhao, M. Hou, S. Jiang, J. Ai, L. Zheng and Z. Shao, *Int. J. Hydrogen Energ.*, 2018, **43**, 2794-2802.

9 Q. Zhao, M. Hou, S. Jiang, J. Ai, L. Zheng and Z. Shao, *J. Electrochem. Soc.*, 2017, **164**, H456-H462.

10 Q. Zhao, M. Hou, S. Jiang, S. Wang, J. Ai, L. Zheng and Z. Shao, *RSC Advances*, 2016, **6**, 80024-80028.

11 A. H. B. Dourado, R. L. Munhos, N. A. Silva, V. D. Colle, G. G. A. Carvalho, P. V. Oliveira, M. Arenz, H. Varela and S. I. Córdoba de Torresi, *ACS Catal.*, 2019, **9**, 8136-8143.